International Journal of Thermophysics, Vol. 25, No. 3, May 2004 (© 2004)

Anomalous Excess Heat Capacities of Ethanol + Alkane Mixtures

J. Peleteiro,[1] **J. Troncoso,**[1] **D. González-Salgado,**[1] **J. L. Valencia,**[1]
C. A. Cerdeiriña,[1] **and L. Romaní**[1, 2]

Received July 7, 2003

A thermodynamic study at atmospheric pressure on the ethanol + *n*-dodecane and ethanol + *n*-tridecane binary systems near their liquid–liquid critical points has been carried out. To this end, densities and speeds of sound were determined in the temperature range from 288.15 to 308.15 K, whereas differential scanning calorimetry was used to obtain isobaric heat capacities per unit volume from 288.15 to 303.15 K as well as liquid–liquid equilibrium curves. All these results for the mentioned properties were obtained over the complete composition range. They were used to obtain molar volumes, isentropic compressibilities, isobaric thermal expansivities, isothermal compressibilities, isochoric heat capacities, and the excess quantities of all these properties. An untypical behavior of the excess heat capacities at the lowest measuring temperatures resulting from the critical behavior of the isobaric heat capacity is observed. No clear anomalies for the excess volumetric properties are detected.

KEY WORDS: density; ethanol + *n*-dodecane; excess properties; heat capacity; speed of sound; upper critical point.

1. INTRODUCTION

The thermodynamic behavior of binary liquid mixtures near liquid–liquid critical points shows strong deviations from ideality. At a microscopic level, this fact arises from the high degree of nonrandomness of the molecular distribution in the mixture, which, ultimately, is responsible for phase

---

[1] Departamento de Física Aplicada, Universidad de Vigo, Facultad de Ciencias del Campus de Ourense, E-32004 Ourense, Spain.
[2] To whom correspondence should be addressed. E-mail: romani@uvigo.es

0195-928X/04/0500-0787/0 © 2004 Plenum Publishing Corporation

separation. This situation is frequently found for (polar + n-alkane) systems, accompanied by a W-shaped composition dependence for the excess isobaric heat capacity $C_{\mathrm{p,m}}^{\mathrm{E}}$ [1–5]. This behavior is a consequence of a variation of the random/nonrandom character of the mixtures with composition—random at the extremes of the composition range and nonrandom at intermediate compositions. Near the critical temperature, the maximum of the curves against composition is strongly enhanced due to the divergence to infinity of the isobaric heat capacity at the critical point. Some recent studies, framed in the study of the thermodynamic properties of nitroalkane + alcohol systems [6, 7], have shown that systems different from (polar + n-alkane) also show, although not W-shaped, a singular composition dependence of $C_{\mathrm{p,m}}^{\mathrm{E}}$ near their critical points.

The 1-alcohol + n-alkane binary systems have been widely studied from both experimental and theoretical points of view [8–14]. Their thermodynamic behavior, concerning deviations from ideality, has been explained in terms of well-known effects at a molecular level. Specifically, the destruction of the self-association structure of pure 1-alcohols accompanied by the change in the nonspecific interactions during mixing produce strong departures from random mixing. Packing effects are also of particular importance with respect to volumetric behavior.

In spite of the large amount of work devoted to alcohol + alkane systems, little is known about their thermodynamic behavior near critical points. This is the purpose of the current work, which is focused on the experimental study of a comprehensive set of excess properties (energetic and volumetric) of ethanol + (n-dodecane and n-tridecane). These systems show critical points that correspond to a maximum and a minimum in the Tx and px equilibrium curves, respectively, i.e., they show phase transitions of the upper critical solution temperature, lower critical solution pressure (UCST, LCSP) type near ambient (working) temperatures. Although other excess properties are studied, the present work is mainly devoted to the excess heat capacity. The high degree of nonrandomness of alcohol + alkane systems far away from the critical point makes the situation interesting in the critical region, where long-range concentration fluctuations occur.

2. EXPERIMENTAL

2.1. Materials

Ethanol (purity > 99.5%) was supplied from Merck, and n-dodecane and n-tridecane (purity > 99%) were supplied from Aldrich. The purities of the products were checked by gas chromatography. All were partially degassed and dried over Fluka type 0.4 nm molecular sieves before use. Mixtures were prepared by weighing to a mole fraction precision of about ± 0.00005 using a Mettler AE-240 balance.

2.2. Equipment

Densities ρ and speeds of sound u were simultaneously measured by using a vibrating-tube densimeter and sound analyzer Anton-Paar DSA-48. Milli-Q water and *n*-heptane were used as calibrating fluids, their values taken from the literature [15–17]. Isentropic compressibilities κ_S were obtained by using density and speed of sound data by means of the Laplace equation $\kappa_S = (\rho u^2)^{-1}$. The repeatability of the measurements is estimated to be $\pm 0.00003\,\mathrm{g \cdot cm^{-3}}$ for ρ and $\pm 0.1\ \mathrm{m \cdot s^{-1}}$ for u, whereas the uncertainty is quoted to $\pm 0.0001\ \mathrm{g \cdot cm^{-3}}$ and $\pm 1\ \mathrm{m \cdot s^{-1}}$. A detailed description of the apparatus and the experimental procedure can be found elsewhere [18].

Isobaric molar heat capacities were obtained from the isobaric heat capacities per unit volume $C_p V^{-1}$, measured with a Setaram Micro DSC II differential scanning calorimeter, and density data. $C_p V^{-1}$ values were determined by the scanning method, whose description was provided in a previous report [19]; *n*-heptane and 1-butanol were used as standard liquids using recommended $C_{p,m}$ values of the compilation of Zabransky et al. [20]. The repeatability of the $C_{p,m}$ measurements was estimated to be about $\pm 0.03\,\mathrm{J \cdot mol^{-1} \cdot K^{-1}}$, whereas, the uncertainty is quoted to $\pm 0.15\,\mathrm{J \cdot mol^{-1} \cdot K^{-1}}$. Liquid–Liquid phase separation temperatures T^* are also determined in heat capacity runs; the procedure involves analysis of the thermogram obtained in a temperature scan [6, 7]. The experiments were performed using a scanning rate of $0.25\,\mathrm{K \cdot min^{-1}}$ resulting in an uncertainty in the T^* determination of about ±0.1 K.

3. RESULTS AND DISCUSSION

3.1. Data Treatment

Figure 1 shows the T^*x curves for the systems of this study. Experimental data are listed in Table I. The solid lines are the fitted curves using the following equations:

$$T^* = T_c + k\,|y - y_c|^{1/\beta}\,, \tag{1}$$

$$y = \frac{\gamma x_1}{1 + x_1(\gamma - 1)} \qquad y_c = \frac{\gamma x_{1,c}}{1 + x_{1,c}(\gamma - 1)}. \tag{2}$$

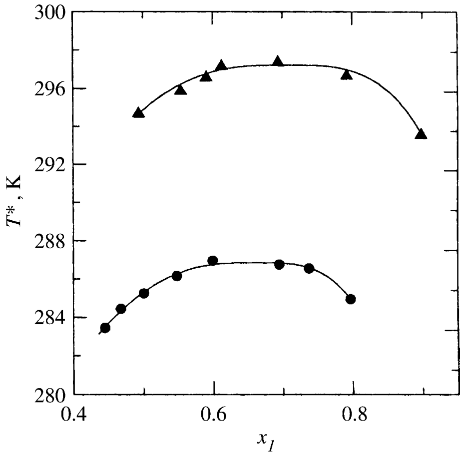

Fig. 1. Liquid–liquid phase separation temperatures T^* for (●) ethanol (1) + *n*-dodecane (2) and (▲) ethanol (1) + *n*-tridecane (2).

β is the critical exponent of the shape of the coexistence curve, fixed at its renormalization group theory value of 0.325 [21]. k, γ, $x_{1,\mathrm{c}}$, and T_c are adjustable parameters, the last two being the coordinates of the

Table I. Liquid–Liquid Phase Transition Temperatures T^*, Fitting Coefficients of Eqs. (1) and (2), and Standard Deviations σ

x_1	T^* (K)	x_1	T^* (K)	x_1	T^* (K)
		Ethanol (1) + *n*-dodecane (2)			
0.44525	283.45	0.54786	286.15	0.73772	286.55
0.46792	284.45	0.59948	286.95	0.79718	284.95
0.50081	285.25	0.69494	286.75		
$x_{1,c}$	T_c (K)	k	γ	σ	
0.6621	286.85	−445.14	0.45857	0.14	
		Ethanol (1) + *n*-tridecane (2)			
0.49408	294.75	0.61340	297.25	0.89850	293.65
0.55454	295.95	0.69415	297.45		
0.59132	296.65	0.79249	296.75		
$x_{1,c}$	T_c (K)	k	γ	σ	
0.7077	297.23	−260.59	0.60400	0.3	

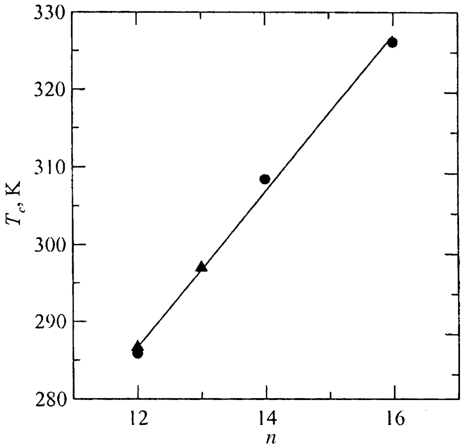

Fig. 2. Critical temperatures T_c for ethanol + C_nH_{n+2} systems: (▲) data obtained in this work; (●) literature data [21]; (—) linear fit.

critical point; their final values are given in Table I. It can be observed that the critical temperature T_c of ethanol + *n*-dodecane is about 10 K lower than that of ethanol + *n*-tridecane. In a previous study [22], an experimental investigation of the liquid–liquid equilibria curves for ethanol + long-chain *n*-alkane systems was performed. The T_c's of this work together with literature values are presented in Fig. 2. Good consistency among them is found; an increment of about 10 K in T_c for each CH_2 group is found (the slope of the straight line is 10.2, in K per CH_2 group). This demonstrates the reliability of our experimental procedure as well as the purity of the chemicals used (for instance, it avoids the presence of small traces of water, that can dramatically affect the value of T_c).

Data of density, speed of sound, and isobaric heat capacity are presented in Tables II, III, and IV, respectively. It must be noted that only data above 293.15 K are given in these tables for ethanol + *n*-tridecane since phase separation takes place between 293.15 and 298.15 K. Isobaric thermal expansivities α_p were obtained from density data at a single temperature (298.15 K for ethanol + *n*-dodecane and 303.15 K for ethanol + *n*-tridecane). Isothermal compressibilities κ_T and isochoric molar heat capacities $C_{v,m}$ were calculated from well-known thermodynamic relations:

$$\kappa_T = \kappa_S + \frac{T V_m \alpha_p^2}{C_{p,m}}, \tag{3}$$

$$C_{v,m} = C_{p,m} \frac{\kappa_S}{\kappa_T}. \tag{4}$$

Values of the above-mentioned properties for the pure liquids as compared to recommended literature data [15] are given in Table V. Overall, the good agreement demonstrates the reliability of the procedures used here. In some cases, the weak disagreement found is explained in terms of internal thermodynamic inconsistencies among recommended data—as an example, for ethanol, the calculated literature value of κ_T using Eq. (3) is $1133\,\mathrm{T\,Pa^{-1}}$, which shows a significant deviation from the reported one ($1153\,\mathrm{T\,Pa^{-1}}$).

Excess quantities were calculated using the Benson and Kiyohara criterion [23], which provides adequate expressions for the ideal value of each thermodynamic property Y. All relevant information about it is given in the following equations:

$$Y^\mathrm{E} = Y - Y^\mathrm{id}, \tag{5}$$

$$V_\mathrm{m}^\mathrm{id} = x_1 V_{\mathrm{m},1}^* + (1 - x_1) V_{\mathrm{m},2}^*, \tag{6}$$

$$C_\mathrm{p,m}^\mathrm{id} = x_1 C_{\mathrm{p,m},1}^* + (1 - x_1) C_{\mathrm{p,m},2}^*, \tag{7}$$

$$\alpha_\mathrm{p}^\mathrm{id} = \phi_1 \alpha_{\mathrm{p},1}^* + (1 - \phi_1) \alpha_{\mathrm{p},2}^*, \tag{8}$$

$$\kappa_\mathrm{T}^\mathrm{id} = \phi_1 \kappa_{\mathrm{T},1}^* + (1 - \phi_1) \kappa_{\mathrm{T},2}^*, \tag{9}$$

$$\kappa_\mathrm{S}^\mathrm{id} = \kappa_\mathrm{T}^\mathrm{id} - \frac{T V_\mathrm{m}^\mathrm{id} (\alpha_\mathrm{p}^\mathrm{id})^2}{C_\mathrm{p,m}^\mathrm{id}}, \tag{10}$$

$$C_\mathrm{v,m}^\mathrm{id} = C_\mathrm{p,m}^\mathrm{id} \frac{\kappa_\mathrm{S}^\mathrm{id}}{\kappa_\mathrm{T}^\mathrm{id}}, \tag{11}$$

$$\phi_1 = x_1 V_{\mathrm{m},1}^* / V_\mathrm{m}^\mathrm{id}, \tag{12}$$

where V_m is the molar volume, ϕ_1 denotes the volume fraction of component 1 (ethanol), and the superscript * denotes properties of the pure liquids.

Results for all excess quantities are plotted in Figs. 3–7. The solid lines in these figures correspond to the fitted values, where Redlich–Kister polynomials were used for this purpose:

$$Y_\mathrm{m}^\mathrm{E} = x_1 (1 - x_1) \sum_{\mathrm{i=0}}^{\mathrm{n}} A_i (2x_1 - 1)^i, \tag{13}$$

$$Y_\mathrm{m}^\mathrm{E} = x_1 (1 - x_1) \sum_{\mathrm{i=0}}^{\mathrm{n}} A_i x^{i/2}. \tag{14}$$

Equation (13) is used to fit all the excess properties with the exception of the excess molar heat capacities, where Eq. (14) was used. The resulting A_i's together with the standard deviations are given in Table VI.

Table II. Densities ρ of the Mixtures at Temperature T (Compositions in Mole Fractions)

	ρ (g · cm^{-3})				
x_1	T=288.15 K	T=293.15 K	T=298.15 K	T=303.15 K	T=308.15 K
Ethanol (1) + n-dodecane (2)					
0	0.75253	0.74888	0.74530	0.74178	0.73833
0.06239	0.75254	0.74883	0.74519	0.74161	0.73809
0.09970	0.75277	0.74905	0.74537	0.74178	0.73824
0.19475	0.75359	0.74981	0.74609	0.74245	0.73886
0.29351	0.75475	0.75093	0.74717	0.74347	0.73982
0.38724	0.75613	0.75227	0.74848	0.74474	0.74102
0.44525	0.75719	0.75332	0.74951	0.74576	0.74205
0.46792	0.75770	0.75381	0.74999	0.74620	0.74247
0.50081	0.75843	0.75452	0.75068	0.74688	0.74312
0.54786	0.75962	0.75570	0.75183	0.74801	0.74423
0.59948	0.76109	0.75714	0.75323	0.74938	0.74556
0.64785	0.76273	0.75874	0.75482	0.75094	0.74709
0.69494	0.76458	0.76056	0.75661	0.75270	0.74884
0.73772	0.76655	0.76251	0.75854	0.75462	0.75076
0.79718	0.76981	0.76573	0.76171	0.75776	0.75386
0.90246	0.77836	0.77419	0.77009	0.76606	0.76209
0.95019	0.78443	0.78023	0.77610	0.77205	0.76804
1	0.79359	0.78931	0.78510	0.78099	0.77692
Ethanol (1) + n-tridecane (2)					
0			0.75264	0.74920	0.74582
0.06505			0.75250	0.74900	0.74555
0.12410			0.75270	0.74915	0.74567
0.22260			0.75323	0.74964	0.74610
0.28439			0.75372	0.75009	0.74651
0.38832			0.75474	0.75108	0.74745
0.40968			0.75503	0.75134	0.74771
0.51156			0.75659	0.75284	0.74916
0.60849			0.75864	0.75484	0.75108
0.68260			0.76064	0.75678	0.75297
0.71552				0.75786	0.75402
0.81832			0.76615	0.76220	0.75832
0.90650			0.77216	0.76817	0.76421
1			0.78510	0.78099	0.77692

Table III. Speeds of Sound u of the Mixtures at Temperature T (Compositions in Mole Fractions)

	u (m·s^{-1})				
x_1	T=288.15 K	T=293.15 K	T=298.15 K	T=303.15 K	T=308.15 K
			Ethanol (1) + n-dodecane (2)		
0	1317.27	1297.66	1278.20	1258.91	1239.82
0.06239	1311.52	1291.75	1272.14	1252.69	1233.74
0.09970	1308.49	1288.70	1268.96	1249.43	1230.06
0.19475	1301.22	1281.41	1261.59	1241.99	1222.53
0.29351	1292.98	1273.21	1253.44	1233.85	1214.39
0.38724	1284.44	1264.67	1244.97	1225.41	1206.18
0.44525	1279.30	1259.52	1239.86	1220.32	1201.23
0.46792	1276.93	1257.15	1237.51	1217.98	1198.95
0.50081	1273.30	1253.47	1233.93	1214.44	1195.47
0.54786	1267.91	1248.24	1228.71	1209.34	1190.24
0.59948	1261.31	1241.75	1222.30	1203.01	1184.12
0.64785	1254.75	1235.24	1215.90	1196.65	1177.71
0.69494	1247.32	1227.92	1208.74	1189.66	1170.89
0.73772	1239.84	1220.63	1201.58	1182.73	1164.12
0.90246	1239.84	1220.63	1201.58	1182.73	1164.12
0.95019	1189.84	1172.09	1154.43	1136.89	1119.87
1	1178.31	1160.97	1143.77	1130.07	1113.07
			Ethanol (1) + n-tridecane (2)		
0			1296.25	1277.13	1258.55
0.06505			1289.30	1270.67	1270.67
0.12410			1284.87	1265.38	1246.61
0.22260			1274.56	1256.93	1256.93
0.28439			1271.64	1252.19	1233.15
0.38832			1261.96	1242.58	1223.68
0.40968			1260.01	1240.66	1221.73
0.51156			1248.88	1229.54	1210.61
0.60849			1236.48	1217.23	1198.40
0.68260			1224.85	1205.31	1186.45
0.71552			1235.01	1200.43	1181.59
0.76697			1215.20	1194.84	1173.15
0.81417			1197.63	1179.15	1161.07
0.90650			1176.33	1155.28	1137.98
1			1143.77	1130.07	1113.07

Table IV. Isobaric Molar Heat Capacities $C_{p,m}$ of the Mixtures at Temperature T (Compositions in Mole Fractions)

	$C_{p,m}$ $(J \cdot mol^{-1} \cdot K^{-1})$			
x_1	$T = 288.15$ K	$T = 293.15$ K	$T = 298.15$ K	$T = 303.15$ K
		Ethanol (1) + *n*-dodecane (2)		
0	370.80	372.99	375.33	377.76
0.05688	363.83	366.80	369.71	372.71
0.06239	362.72	365.75	368.76	371.74
0.09970	354.82	357.93	361.53	364.99
0.19475	330.88	334.56	338.46	342.32
0.29351	304.94	308.64	312.46	316.40
0.38724	280.47	283.72	287.64	291.58
0.44525	265.04	268.13	271.98	275.78
0.46792	258.84	262.06	265.72	269.40
0.50081	250.07	253.12	256.63	260.13
0.54786	237.42	240.29	243.72	247.16
0.59948	223.58	225.74	229.00	232.46
0.69494	197.03	199.25	201.74	205.47
0.73772	184.60	186.91	189.65	192.62
0.79718	167.24	169.67	172.35	175.26
0.90246	136.38	138.69	141.18	143.71
0.95019	122.52	124.57	126.72	128.98
1	108.27	110.06	112.01	114.00
		Ethanol (1) + *n*-tridecane (2)		
0			402.29	404.83
0.06505			397.48	400.63
0.12868			381.44	385.02
0.29690			333.64	337.33
0.39373			304.86	308.60
0.40313			302.13	305.93
0.49408			274.94	278.41
0.55454			256.25	
0.59132			245.43	248.21
0.61341			238.55	242.32
0.69415			213.91	215.95
0.79249			181.43	183.92
0.8985			145.57	148.07
0.95133			127.99	130.20
1			112.00	114.00

Table V. Thermodynamic Properties of the Pure Liquids at Temperature T

		ρ (g · cm^{-3})		$C_{p,m}$ (J · mol^{-1} · K^{-1})		α_p (k K^{-1})		κ_T (T Pa^{-1})		κ_s (T Pa^{-1})	
Liquid	T (K)	This work	Ref. 15	This work	Ref. 15	This work	Ref. 15	This work	Ref. 15	This work	Ref. 15
Ethanol	288.15	0.79359	0.79360								
	293.15	0.78931	0.78920								
	298.15	0.78510	0.78493	112.01	112.34	1.061	1.096	1150	1153	973.73	946
n-Dodecane	293.15	0.74888	0.74875								
	298.15	0.74530	0.74518	375.33	375.97	0.954	0.974	987		821.37	816.03
n-Tridecane	308.15	0.75264	0.75271	402.29	406.89	0.912	0.950	942		790.67	786.03

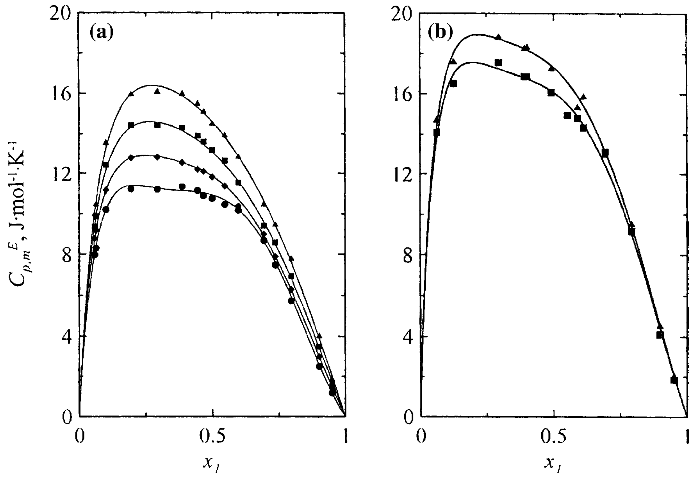

Fig. 3. Excess isobaric molar heat capacities $C^{E}_{p,m}$ for (a) ethanol (1) + *n*-dodecane (2) at the temperatures (●) 288.15 K, (◆) 293.15 K, (■) 298.15 K, and (▲) 303.15 K and (b) ethanol (1) + *n*-tridecane (2) at the temperatures (■) 298.15 K, and (▲) 303.15 K. (—) Fitted values from Eq. (14).

3.2. Excess Heat Capacities

Figure 3 shows the excess isobaric molar heat capacities. They are large and positive over the complete composition range and increase with temperature for both systems (typical for strongly associated mixtures). Such behavior can be easily explained from the partial breaking of the hydrogen-bonding structure of ethanol during mixing. More specifically, the fact that hydrogen bonds even exist in solution makes the structure of the mixtures to be weaker than that of pure ethanol. Thus, order decreases with temperature more rapidly for mixtures. Taking into account that $C_{\mathrm{p,m}} = T\,(\partial S_{\mathrm{m}}/\partial T)_{\mathrm{p}}$, this results in a positive contribution to $C^{\mathrm{E}}_{\mathrm{p,m}}$.

The composition dependence of $C^{\mathrm{E}}_{\mathrm{p,m}}$ reveals the critical behavior of the heat capacity of the mixture. Normally, $C^{\mathrm{E}}_{\mathrm{p,m}}$ for alcohol + alkane systems shows curves with a maximum located in the *n*-alkane-rich region. As shown in Fig. 3a, this behavior is exhibited for ethanol + *n*-dodecane at the highest experimental temperature. As the temperature decreases, the curves become flat, resulting in an inflection point at medium-to-high mole fractions. This constitutes an untypical behavior of the $C^{\mathrm{E}}_{\mathrm{p,m}}$ of alcohol + alkane systems, which would be more important in the immediate proximity of T_c, where a M-shaped $C^{\mathrm{E}}_{\mathrm{p,m}}(x)$ curve is expected to

Table VI. Fitting Coefficients A_i of Eqs. (13) and (14) and Standard Deviations σ

T (K)	A_1	A_2	A_3	A_4	A_5	A_6	A_7	σ
Ethanol (1) + dodecane (2)								
V_m^E (cm^3 · mol^{-1})								
288.15	1.8736	0.0279	0.5392	1.0939	1.9775	−1.0066		0.004
293.15	2.0105	0.0059	0.5760	1.0049	2.1283	−1.0526		0.004
298.15	2.1378	−0.0043	0.6941	0.7915	2.1298	−0.8931		0.004
303.15	2.2724	−0.0287	0.7244	0.8409	2.1295	−1.0258		0.005
308.15	2.4201	0.0655	0.7370	−0.0233	2.1165			0.008
$C_{p,m}^E$ (J · mol^{-1} · K^{-1})								
288.15	314.14	−851.98	573.09	477.94	−494.88			0.13
293.15	366.72	−1160.18	1435.14	−613.01				0.09
298.15	373.64	−1113.69	1319.47	−546.51				0.16
303.15	379.33	−1067.25	1204.56	−477.10				0.18
α_p^E (MK^{-1})								
298.15	178.0	60.0	108.9					1.2
κ_T^E (T Pa^{-1})								
298.15	116.6	79.2	120.0	17.6	-136.7	157.6	313.3	0.3
κ_S^E (T Pa^{-1})								
298.15	89.0	55.7	92.6	36.0	-59.9	116.5	240.0	0.15
$C_{v,m}^E$ (J · mol^{-1} · K^{-1})								
298.15	318.98	−946.63	1089.66	−433.02				0.14
Ethanol (1) + *n*-tridecane (2)								
V_m^E (cm^3 · mol^{-1})								
298.15	2.0483	−0.1005	0.3744	0.7462	2.4351			0.006
303.15	2.1993	−0.0795	0.5093	0.6058	2.3305			0.004
308.15	2.3682	−0.0943	0.6093	0.4745	2.3321			0.006
$C_{p,m}^E$ (J · mol^{-1} · K^{-1})								
298.15	579.24	−1954.87	2532.42	−1153.15	35.68			0.4
303.15	586.54	−1924.02	2432.63	−1055.08				0.3
α_p^E (MK^{-1})								
303.15	196.320	89.467	147.865					1.5
κ_T^E (T Pa^{-1})								
303.15	111.62	76.62	106.11	47.26	68.48	104.16		0.4
κ_S^E (T Pa^{-1})								
303.15	85.50	50.16	74.28	51.01	97.96	65.08		0.2
C_v^E (J · mol^{-1} · K^{-1})								
303.15	521.96	−1734.08	2191.31	−948.52				0.12

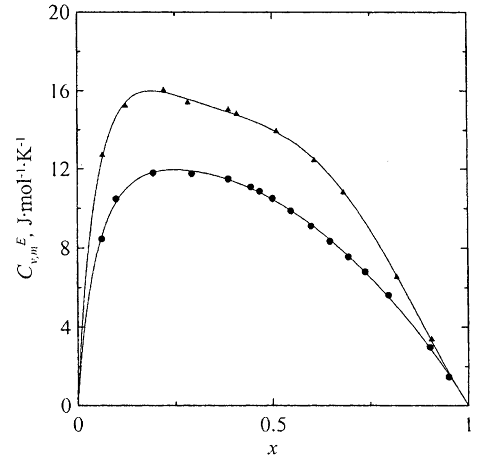

Fig. 4. Excess isochoric molar heat capacities $C_{\mathrm{v,m}}^{\mathrm{E}}$ for (●) ethanol (1) + *n*-dodecane (2) at 298.15 K and (▲) ethanol (1) + *n*-tridecane (2) at 303.15 K. (—) Fitted values from Eq. (14).

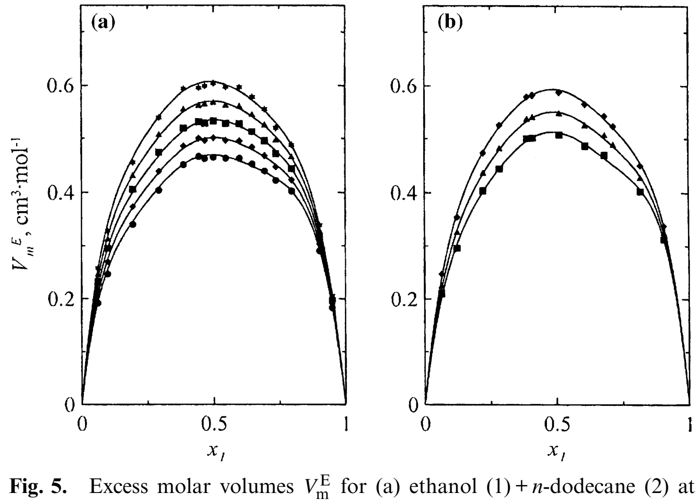

Fig. 5. Excess molar volumes $V_{\mathrm{m}}^{\mathrm{E}}$ for (a) ethanol (1) + *n*-dodecane (2) at the temperatures (●) 288.15 K, (◆) 293.15 K, (■) 298.15 K, (▲) 303.15 K and (⋆) 308.15 K and (b) ethanol (1) + *n*-tridecane (2) at the temperatures (■) 298.15 K, (▲) 303.15 K and (⋆) 308.15 K. (—) Fitted values from Eq. (13).

appear. The new maximum would be located near the critical composition ($x_{\mathrm{C}} = 0.6621$) as a result of the critical behavior of C_{p}. It is well-known [21] that the isobaric heat capacity of a mixture diverges to infinity at the

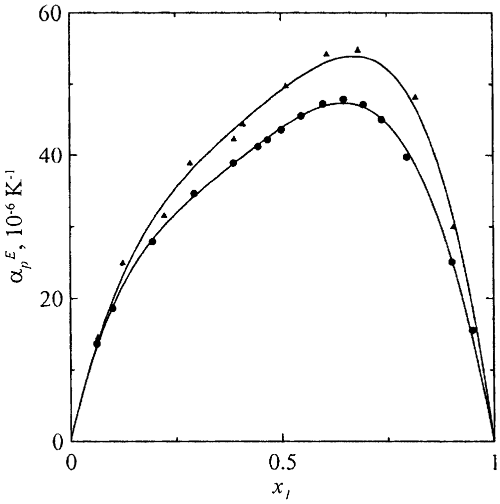

Fig. 6. Excess isobaric thermal expansivities for: (●) ethanol (1) + n-dodecane (2) at 298.15 K and (▲) ethanol (1) + n-tridecane (2) at 303.15 K. (—) Fitted values from Eq. (13).

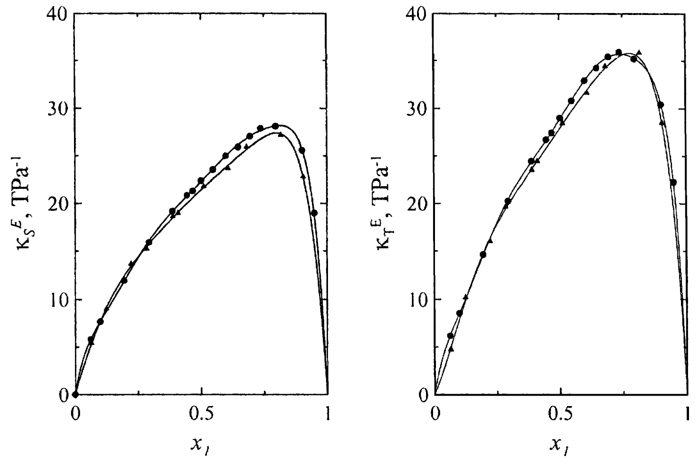

Fig. 7. Excess isentropic κ_s^E and isothermal κ_T^E compressibilities for (●) ethanol (1) + n-dodecane (2) at 298.15 K and (▲) ethanol (1) + n-tridecane (2) at 303.15 K (—). Fitted values from Eq. (13).

liquid–liquid critical point according to a power law of the type,

$$C_p = \frac{A^{\pm}}{\alpha}\left|\frac{T-T_c}{T_c}\right|^{-\alpha}, \tag{15}$$

where A is the critical amplitude and α is the critical exponent. The superscripts + and − in Eq. (15) refer to the homogeneous and heterogeneous regions, respectively. Usually, the effect of the critical behavior of C_p in $C_{p,m}^E$ is more remarkable than that observed here [5–7]. Thus, a small critical anomaly in C_p for this system is expected. A values can be obtained from calorimetry or, indirectly, from data of the correlation length ξ as obtained from light scattering experiments. As C_p, ξ follows a power law,

$$\xi = \xi_0^{\pm} \left| \frac{T - T_c}{T_c} \right|^{-\nu}. \tag{16}$$

According to the two-scale factor universality (modern theory of critical phenomena [21]), there exists a universal dimensionless parameter $X = A^{+}(\xi_0^{+})^3/k_B$ relating A^{+} with the critical amplitude of the correlation length ξ_0^{+}, with K_B denoting the Boltzmann constant. A previous study [24] reveals a large value of ξ_0^{+} for this system, which explains the small anomaly in C_p. Another point that must be stressed is that the regular contribution to $C_{p,m}^E$ is large for this type of mixture and masks the critical contribution. The behavior of the $C_{p,m}^E$ of ethanol + *n*-tridecane system (Fig. 3b) as well as that of the $C_{v,m}^E$ for both systems (Fig. 4) is in accordance with the previous assertions.

3.3. Excess Volumetric Properties

The excess molar volumes, shown in Fig. 5, are positive over the complete composition range, and they increase with temperature for both systems. Positive contributions, arising from nonspecific interactions and hydrogen-bond rupture during mixing, dominate the negative ones (packing effects). The latter are expected to be important when the working range is near the critical temperature of the *n*-alkane. This makes *n*-alkane molecules to be gas-like, resulting in contraction upon mixing. Since critical temperatures of *n*-dodecane and *n*-tridecane are 658.3 and 675.8 K, respectively, it appears reasonable that packing hardly contributes to the excess molar volumes for both systems. It must be noted that, for near-critical temperatures, $V_m^E(x)$ curves are flattened around x_c as a consequence of the diverging behavior of α_p at the critical point. Excess isobaric thermal expansivities α_p^E are presented in Fig. 6. They are positive over the complete composition range. The maxima of the curves are located near the critical composition, suggesting a possible influence of the nearness to the critical point on α_p^E. Then, it can be concluded that this behavior could represent a very small critical anomaly (no clear composition anomaly is detected) for the studied systems. Finally, the excess compressibilities κ_s^E and κ_T^E are shown in Fig. 7. The positive values of both properties come from the net hydrogen-bond rupture, which makes the mixtures more compressible than pure liquids. Although κ_T^E is a property that must diverge at the critical point, there is no evidence of critical anomalies for the studied systems. Larger anomalies can be expected for alcohol + alkane systems with small ξ_0^+. This is the case for methanol + *n*-heptane; a detailed study of the behavior of α_p for this system can be found elsewhere [21].

ACKNOWLEDGMENTS

This research is partially supported by the Dirección General de Investigación, Ministerio de Ciencia y Tecnología of Spain (Grant No. BFM2000-0597 of the Programa Nacional de Promoción General del Conocimiento). Authors are also indebted to the Dirección Xeral de Ordenación Universitaria e Política Científica (Xunta de Galicia, Grant No. PGIDT01PXI38304PN) for financial support.

REFERENCES

1. H. Kalali, F. Kohler, and P. Svejda, *Fluid Phase Equilib.* **20**:75 (1985).
2. M-E. Saint-Victor and D. Patterson, *Fluid Phase Equilib.* **35**:237 (1987).
3. R. G. Rubio, M. Cáceres-Alonso, R. M. Masegosa, L. Andreolli-Ball, M. Costas, and D. Patterson, *Ber Bunsenges Phys. Chem.* **93**:48 (1989).
4. L. M. Trejo, M. Costas, and D. Patterson, *J. Chem. Soc. Faraday Trans.* **87**:3001 (1991).
5. C. A. Tovar, E. Carballo, C. A. Cerdeiriña, M. I. Paz Andrade, and L. Romaní, *J. Chem. Soc. Faraday Trans.* **93**:3505 (1997).
6. C. A. Cerdeiriña, C. A. Tovar, E. Carballo, J. Troncoso, and L. Romaní, *Int. J. Thermophys.* **21**:1419 (2000).
7. C. A. Cerdeiriña, C. A. Tovar, D. González, E. Carballo, and L. Romaní, *Fluid Phase Equilib.* **179**:101 (2001).
8. Y. Brown, W. Fock, and F. Smith, *Aust. J. Chem.* **17**:1106 (1964).
9. A. J. Treszczanowicz, O. Kiyohara, and G. C. Benson, *J. Chem. Thermodyn.* **13**:253 (1981).
10. M. Costas and D. Patterson, *J. Chem. Soc. Faraday Trans.* **81**:379 (1985).
11. J. B. Ott, P. R. Brown, and J. T. Sipowska, *J. Chem. Thermodyn.* **28**:379 (1996).
12. J. B. Ott and J. T. Sipowska, *J. Chem. Eng. Data* **41**:987 (1996).
13. J. Peleteiro, D. González-Salgado, C. A. Cerdeiriña, J. L. Valencia, and L. Romaní, *Fluid Phase Equilib.* **191**:83 (2001).
14. J. Peleteiro, D. González-Salgado, C. A. Cerdeiriña, and L. Romaní, *J. Chem. Thermodyn.* **34**:485 (2002).
15. J. A. Riddick, W. B. Bunger, and T. Sakano, *Organic Solvents. Physical Properties and Methods of Purification*, Vol. II (Wiley, New York, 1986).
16. I. Cibulka, *Fluid Phase Equilib.* **89**:1 (1993).
17. N. Bilaniuk and G. S. K. Wong, *J. Acoust. Soc. Am.* **93**:1609 (1993).

18. J. Troncoso, E. Carballo, C. A. Cerdeiriña, D. González, and L. Romaní, *J. Chem. Eng. Data* **45**:594 (2000).
19. C. A. Cerdeiriña, J. A. Míguez, E. Carballo, C. A. Tovar, E. de la Puente, and L. Romaní, *Thermochim. Acta* **347**:37 (2000).
20. M. Zabransky, V. Ruzicka, V. Mayer, and E. S. Domalski, *J. Phys. Chem. Ref. Data (Monograph No. 6), Heat Capacities of Liquids, Critical Review and Recommended Values* (1996).
21. A. Kumar, H. R. Krishnamurthy, and E. S. R. Gopal, *Phys. Rep.* **98**:57 (1983).
22. U. Dahlmann and G. M. Schneider, *J. Chem. Thermodyn.* **21**:997 (1989).
23. G. C. Benson and O. Kiyohara, *J. Chem. Thermodyn.* **11**:1061 (1979).
24. U. Dürr, S. Z. Mirzaev, and U. Kaatze, *J. Phys. Chem. A* **104**:8855 (2000).